

This document is the Accepted Manuscript version of a Published Work that appeared in final form in Analytical Chemistry, copyright © American Chemical Society after peer review and technical editing by the publisher. To access the final edited and published work see <http://pubs.acs.org/doi/full/10.1021/acs.analchem.6b01802>".

Supporting Information

Numerical simulation and experimental validation of calibrant-loaded extraction phase standardization approach

Md. Nazmul Alam, Janusz Pawliszyn*

Department of Chemistry, University of Waterloo, Waterloo, Ontario, N2L 3G1, Canada

*Corresponding Author

Tel.:+1-519-888-4641. Fax: + 519 746 0435

E-mail:janusz@uwaterloo.ca

Figure or Table	Page #
Figure S1. The geometrical configuration of the SPME-sample system used in the computational model.	S-3
Figure S2. Effect of variation of diffusion coefficients (D_s) on desorption kinetics	S-4
Figure S3. Experimental desorption rate constant (a_d) of some analytes with respect to their partition coefficient (K_{es}).	S-5
Figure S4. Effect of fluid flow velocity on the desorption kinetics.	S-6
Figure S5. (a) Effect of matrix concentration on desorption kinetics in infinite volume case. $K_{es} = 100$, $K_a = 1 \times 10^5$ liter/kg, $k_d = 1$ [1/s] (labile). (b) The variation of a_d of pyrene with a wide range of BSA concentrations at two different fluid flow velocities	S-7
Figure S6. Effect of matrix concentration on desorption kinetics in finite volume case.	S-8
Figure S7. The variation of rate constants of sorption and desorption under different experimental conditions, such as presence of a binding matrix, different fluid velocity.	S-8
Figure S8. Computational simulation result shows iso-symmetry of fraction remaining (Q/q_0) of calibrant and normalized extraction amount (n/n_e) of analyte.	S-9
Table S1. Standard loaded calibration with the equation (4, main text) to get free concentration with the use of K_{es} (10,000) obtained from a binding-matrix free sample solution.	S-10
Table S2 Standard loaded calibration with the equation (4, main text) to get total concentration with the use of K_{es} (99.53) obtained from a binding-matrix containing sample solution	S-10
Figure S9. Calibration curve with the ratio of extracted amount (n) and remaining calibrant (Q) at a particular point of extraction time profile	S-11
Table S3. Determination of the limits of analyte K_{es} that can be calibrated with one-calibrant loaded SPME (one-CL-SPME) using eq. 7	S-12
Table S4. Determination of the limits of analyte K_{es} that can be calibrated with one-calibrant loaded SPME (one-CL-SPME) using eq. 8	S-12
Table S5. Effect of association constants of analytes (K_a^A) on the accuracy of the one calibrant equations (eq. 9).	S-13
Table S6. Quantitative evaluation of the correspondence between the numerical model and the experimental data.	S-13

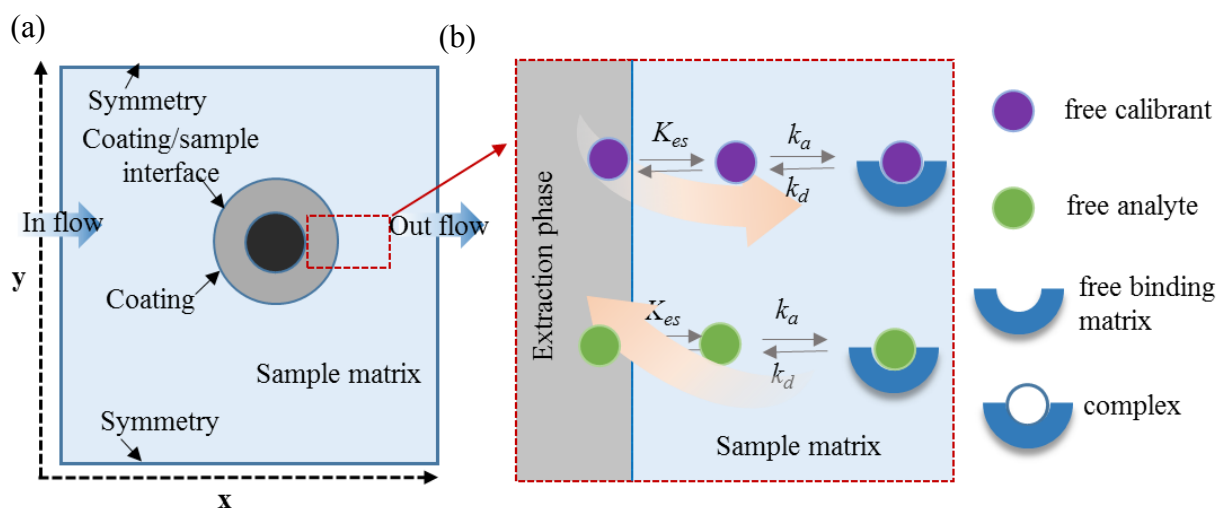


Figure S1. a) The geometrical configuration of the SPME-sample system used in the computational model. SPME consists of some durable structure (black) coated with a thin layer of polymer. The coating is in contact with the sample matrix. b) The interaction process in matrix-analyte-SPME system. Calibrant (purple) pre-loaded to the coating transported from the coating via diffusion to the sample matrix where it is subject to diffusion and convection in its free phase and may bind to specific binding sites of matrix components. Analytes (green) present in the sample either free or bound to the matrix transports to the coating where only free analyte is extracted. Diagram is not to scale.

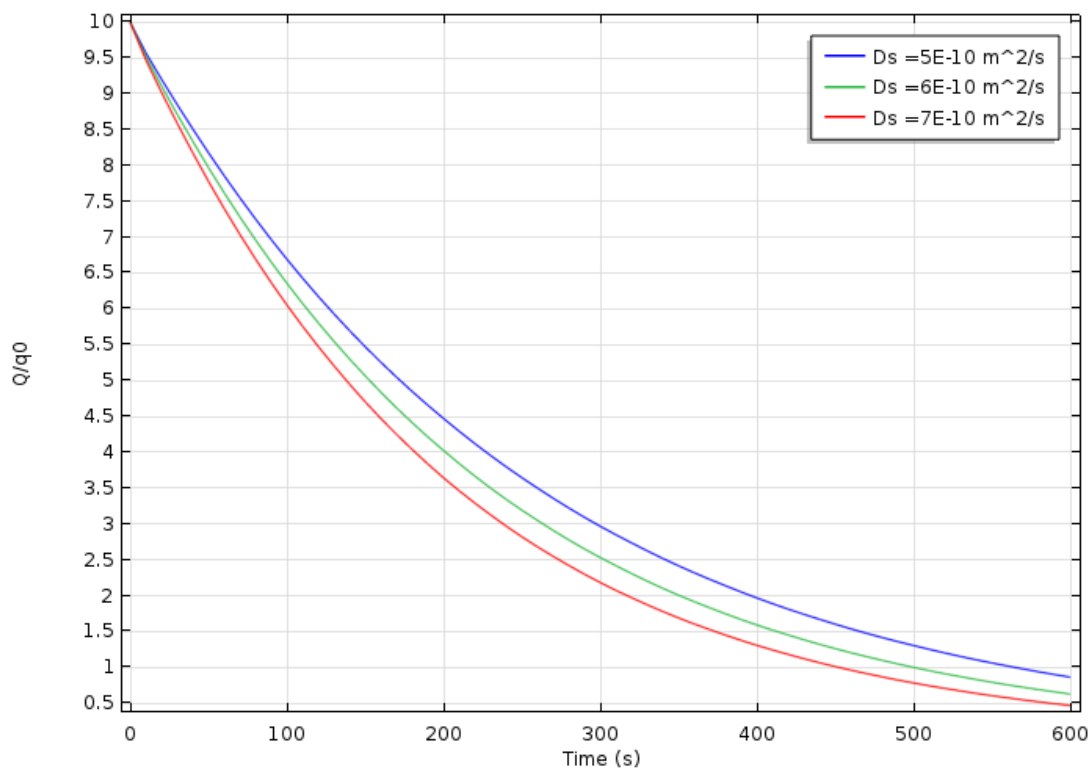


Figure S2. Effect of variation of diffusion coefficients (D_s) on desorption kinetics. Partition coefficients (K_{es}) are assumed to be constant at 100 and diffusion coefficient in the extraction phase is $1/6^{\text{th}}$ of D_s , volume of the sample was considered infinite. All other conditions were same as Figure 1 (main paper).

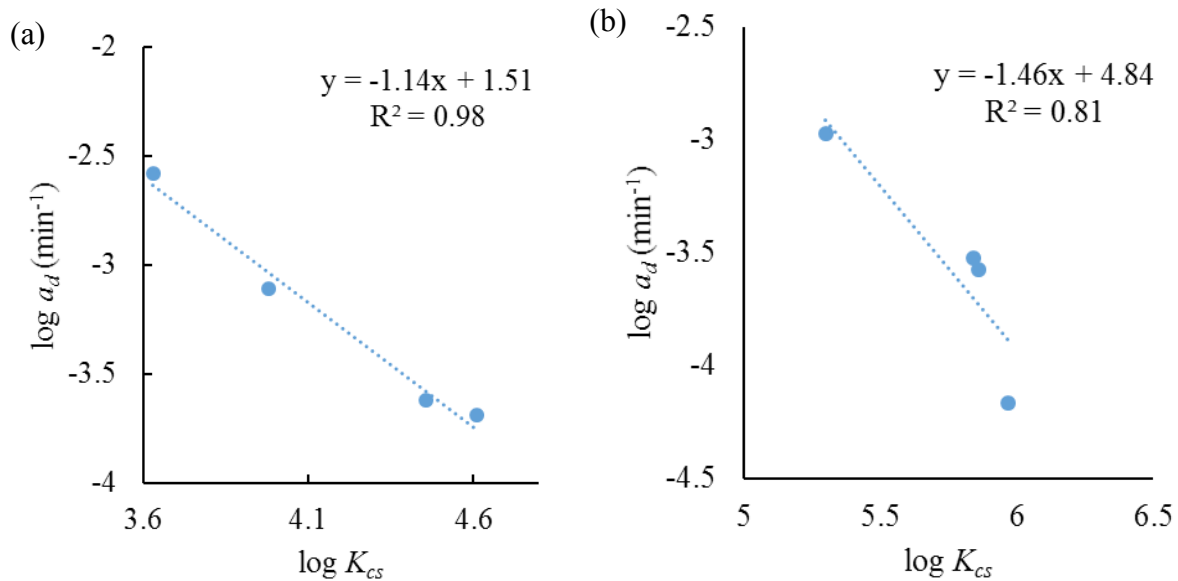


Figure S3. Experimental desorption rate constant (a_d) of some analytes with respect to their partition coefficient (K_{cs}). (a) Data obtained from Ouyang et al.¹ (b). Data obtained from Cui et al.²

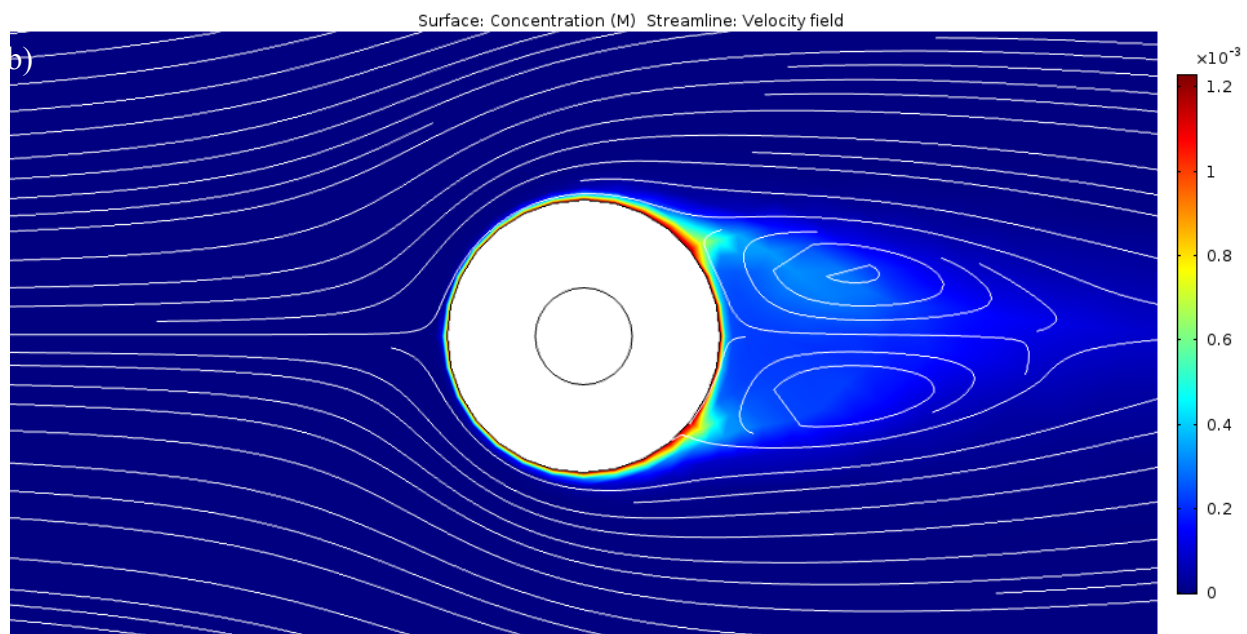
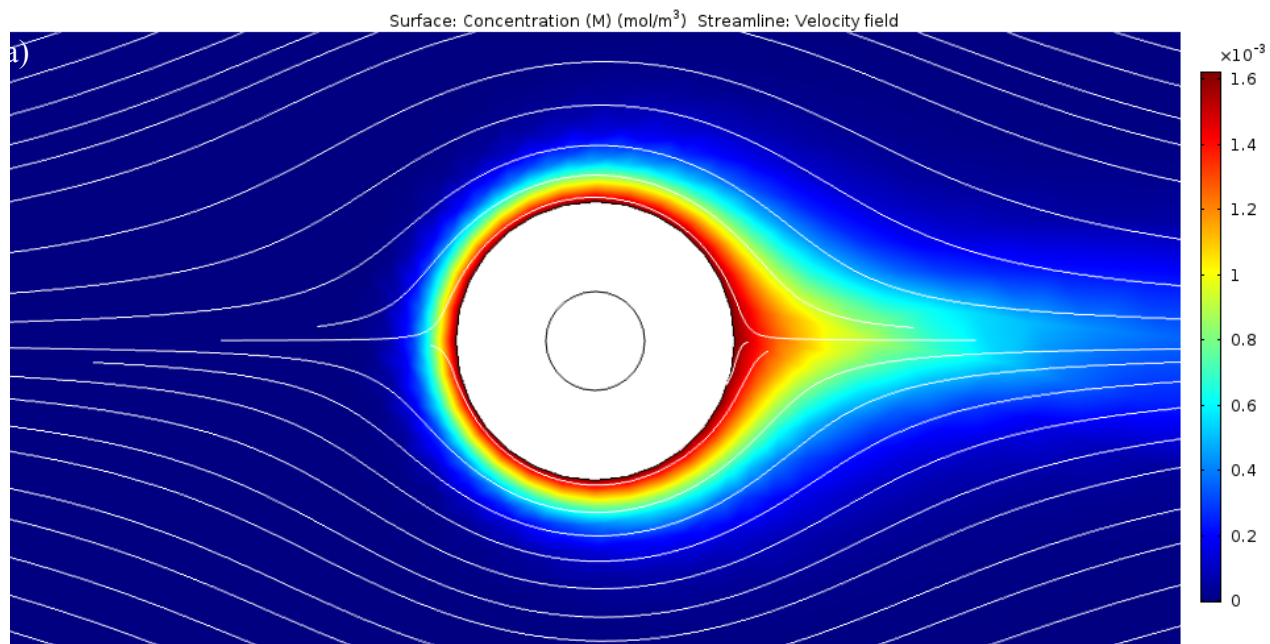


Figure S4. Effect of fluid flow velocity on the desorption kinetics. Surface plot shows the concentration (mol L^{-1}) of calibrant desorbed from the extraction phase and the

streamline is for the velocity field. Fluid velocity (a) 0.1 cm s^{-1} , and (b) 1 cm s^{-1} .

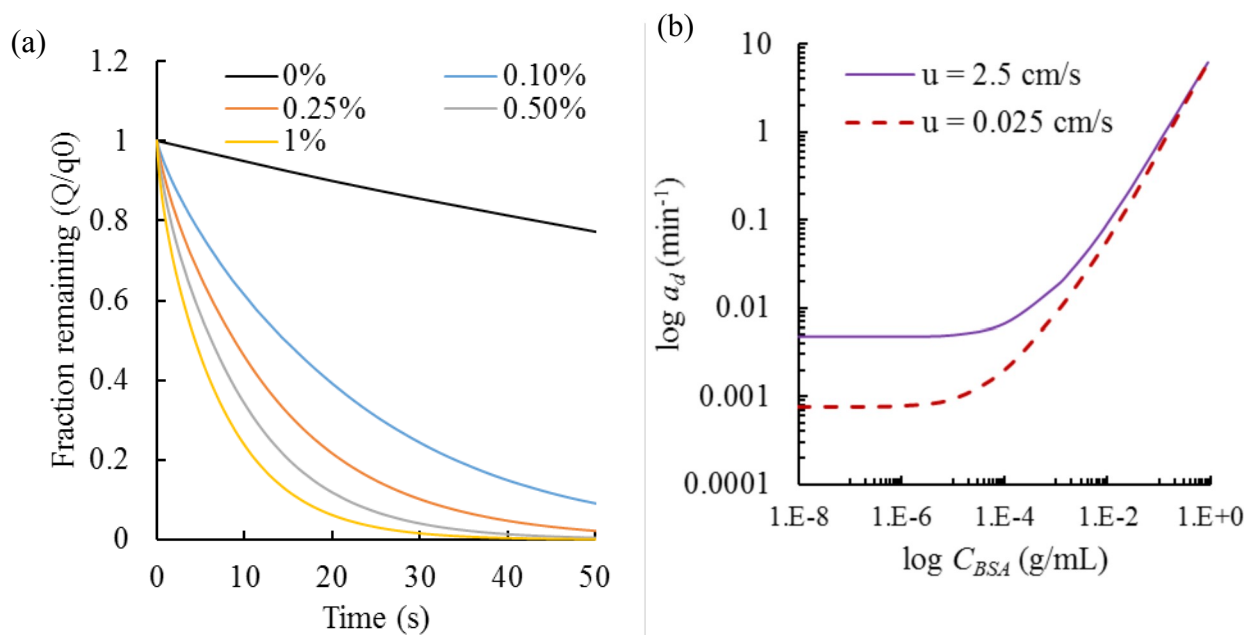


Figure S5. (a) Effect of matrix concentration on desorption kinetics in infinite volume case. $K_{es} = 100$, $K_a = 1 \times 10^5 \text{ liter/kg}$, $k_d = 1 \text{ [1/s]}$ (labile). (b) The variation of a_d of pyrene with a wide range of BSA concentrations at two different fluid flow velocities

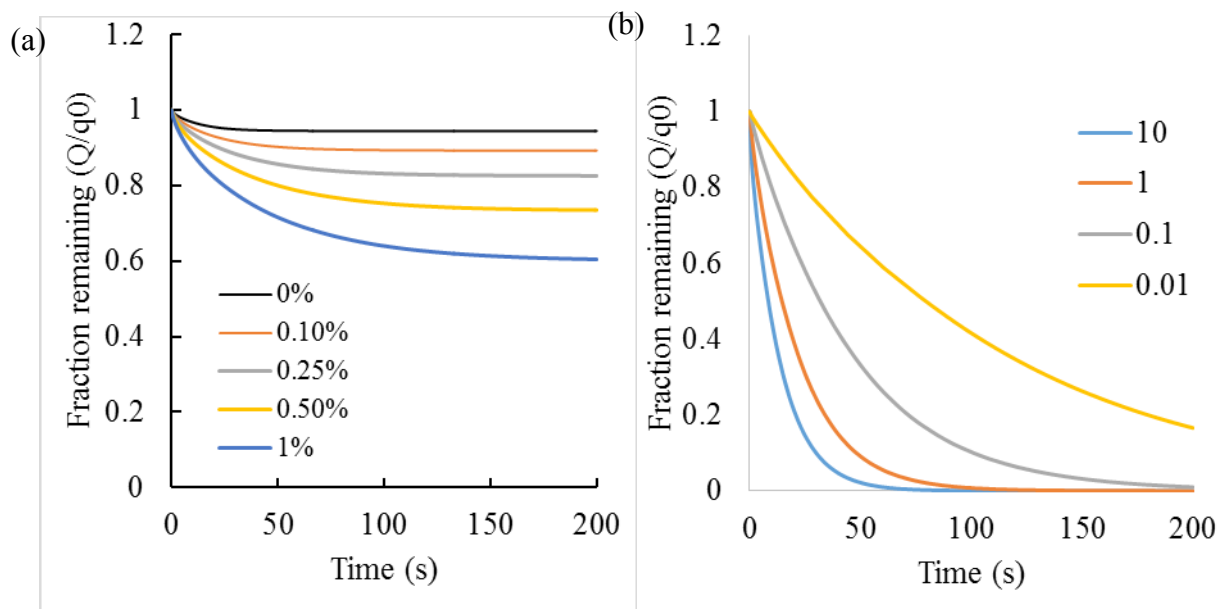


Figure S6. Effect of matrix concentration on desorption kinetics in finite volume case. (a) $K_a = 1 \times 10^3$ liter/kg, $k_d = 1$ s⁻¹ (labile). (b) Effect of k_d on the desorption kinetics at infinite sample volume.

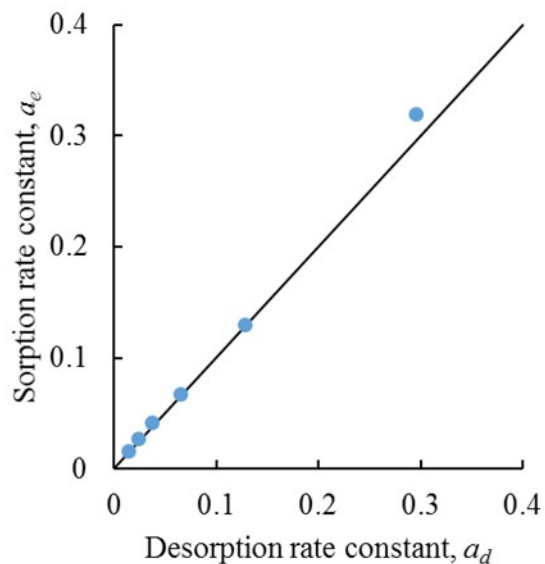


Figure S7. The variation of rate constants of sorption and desorption under different experimental conditions, such as presence of a binding matrix, different fluid velocity.

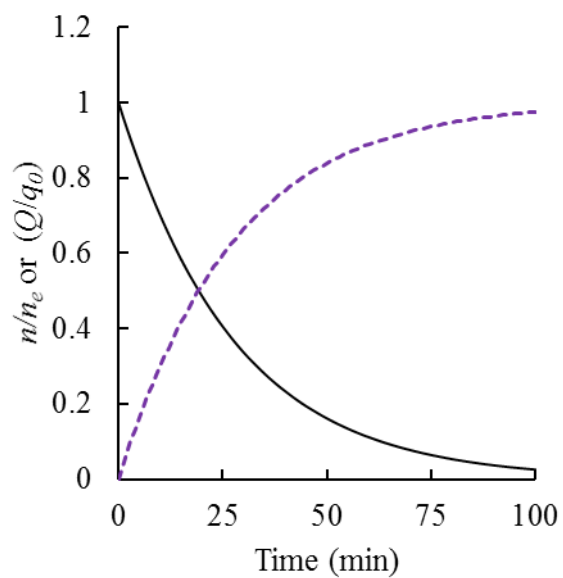


Figure S8. Computational simulation result shows iso-symmetry of fraction remaining (Q/q_0) of calibrant and normalized extraction amount (n/n_e) of analyte. $C_A^0 = 50 \text{ ng ml}^{-1}$, $C_M = 0.001 \text{ g ml}^{-1}$, $K_{es} = 10,000$, $K_a = 1 \times 10^5$, $V_e = 1.8 \times 10^{-4} \text{ ml}$, fluid velocity = 0.1 cm s^{-1} . Physical properties of the analyte and its calibrant is assumed same.

Table S1. Standard loaded calibration with the equation (4, main text) to get **free** concentration with the use of K_{es} (10,000) obtained from a binding-matrix free sample solution.

True concentration		In silico results					
Cs (ng/mL) (True, total)	Cs (ng/mL) (True, Free)	Sampling time (min)	extracted amount, ng	Q/q0	Cs (ng/mL) (insilco)	Conc. Obtained	Bias
50	0.495	5	0.1461	0.8374	0.499	Free	-0.84%
		10	0.2692	0.7000	0.498	Free	-0.67%
		20	0.4604	0.4864	0.498	Free	-0.59%
		80	0.8480	0.0535	0.498	Free	-0.53%

Table S2 Standard loaded calibration with the equation (4, main text) to get **total** concentration with the use of K_{es} (99.53) obtained from a binding-matrix containing sample solution

True concentration		In silico results					
Cs (ng/mL) (True, total)	Cs (ng/mL) (True, Free)	Sampling time (min)	extracted amount, ng	Q/q0	Cs (ng/mL) (insilco)	Conc. Obtained	Bias
50	0.49507	5	0.1461	0.837	50.2	Total	-0.32%
		10	0.2692	0.700	50.1	Total	-0.15%
		20	0.4604	0.486	50.0	Total	-0.07%
		80	0.8480	0.053	50.0	Total	-0.01%

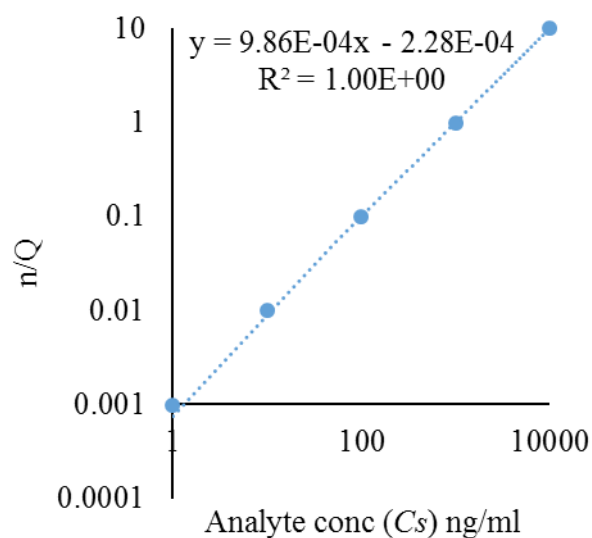


Figure S9. Calibration curve with the ratio of extracted amount (n) and remaining calibrant (Q) at a particular point of extraction time profile, all conditions are same as Figure 1. The sampling time can be either in linear part or at equilibrium. With 50 ng ml^{-1} sample solution and 10 ng calibrant loaded on SPME coating, the n/Q was 0.0492 ng, by using the calibration curve (Figure 2) the in-silico concentration is 50.16, the bias is 0.3 %. Therefore the concentration obtained in this approach is TOTAL concentration.

Table S3. Determination of the limits of analyte K_{es} that can be calibrated with one-calibrant loaded SPME (one-CL-SPME) using eq. 7 [D_s^A values obtained from Vrana et.al.³

Analytes	K_{es}^A	$D_s^A \times 10^6 \text{ cm}^2/\text{s}$	$a_e \text{ (s}^{-1}\text{)}$		% Error	Naphthalene eq. 7 $a_e \text{ s}^{-1}$	%Error	Eq. 7 Fluoranthene $a_e \text{ s}^{-1}$	% Error
			Numerical simulation	Chrysene Eq. 7					
Naphthalene	1047	7.5	1.4×10^{-4}	1.7×10^{-4}	20	1.4×10^{-4}	0	1.6×10^{-4}	13
Acenaphthene	4266	6.34	3.2×10^{-5}	3.6×10^{-5}	11	3.0×10^{-5}	7	3.4×10^{-5}	5
Fluorene	5129	6.04	2.6×10^{-5}	2.8×10^{-5}	10	2.4×10^{-5}	8	2.7×10^{-5}	3
Anthracene	9550	5.88	1.4×10^{-5}	1.5×10^{-5}	8	1.2×10^{-5}	10	1.4×10^{-5}	2
Benzo[ghi]perylene	19055	4.81	5.9×10^{-6}	6.1×10^{-6}	2	5.0×10^{-6}	15	5.7×10^{-5}	4
Indeno[1,2,3-cd]pyrene	26915	4.88	4.3×10^{-6}	4.4×10^{-6}	2	3.6×10^{-6}	15	4.1×10^{-6}	4
Fluoranthene	51286	5.55	2.4×10^{-6}	2.6×10^{-6}	6	2.2×10^{-6}	11	2.4×10^{-6}	0
Pyrene	72444	5.6	1.8×10^{-6}	1.9×10^{-6}	6	1.5×10^{-6}	12	1.7×10^{-6}	0
Benz[a]anthracene	181970	5.13	6.7×10^{-7}	6.8×10^{-7}	2	5.6×10^{-7}	15	6.4×10^{-7}	4
Benzo[a]pyrene	245471	4.96	4.7E-07	4.9×10^{-7}	3	4.0×10^{-7}	14	4.6×10^{-7}	3
Chrysene	489779	5.1	2.5E-07	2.5×10^{-7}	0	2.1×10^{-7}	17	2.4×10^{-7}	6

Table S4. Determination of the limits of analyte K_{es} that can be calibrated with one-calibrant loaded SPME (one-CL-SPME) using eq. 8 [D_s^A values obtained from Vrana et.al.³

Analytes	K_{es}^A	$D_s^A \times 10^6 \text{ cm}^2/\text{s}$	$a_e \text{ (s}^{-1}\text{)}$		% Error	Naphthalene eq. 7 $a_e \text{ s}^{-1}$	%Error	Eq. 7 Fluoranthene $a_e \text{ s}^{-1}$	% Error
			Numerical simulation	Chrysene Eq. 7					
Naphthalene	1047	7.5	1.4×10^{-4}	1.5×10^{-4}	4	1.4×10^{-4}	0	1.4×10^{-4}	1
Acenaphthene	4266	6.34	3.2×10^{-5}	3.3×10^{-5}	3	3.2×10^{-5}	1	3.2×10^{-5}	0
Fluorene	5129	6.04	2.6×10^{-5}	2.7×10^{-5}	3	2.6×10^{-5}	1	2.6×10^{-5}	0
Anthracene	9550	5.88	1.4×10^{-5}	1.4×10^{-5}	3	1.4×10^{-5}	1	1.4×10^{-5}	0
Benzo[ghi]perylene	19055	4.81	5.9×10^{-6}	6.2×10^{-6}	4	6.0×10^{-6}	1	6.0×10^{-5}	1
Indeno[1,2,3-cd]pyrene	26915	4.88	4.3×10^{-6}	4.4×10^{-6}	4	4.3×10^{-6}	0	4.3×10^{-6}	1

Fluoranthene	51286	5.55	2.4×10^{-6}	2.5×10^{-6}	3	2.4×10^{-6}	1	2.4×10^{-6}	0
Pyrene	72444	5.6	1.8×10^{-6}	1.8×10^{-6}	2	1.7×10^{-6}	1	1.7×10^{-6}	1
Benz[a]anthracene	181970	5.13	6.7×10^{-7}	6.8×10^{-7}	21	6.5×10^{-7}	2	6.6×10^{-7}	2
Benzo[a]pyrene	245471	4.96	4.7E-07	4.9×10^{-7}	3	4.7×10^{-7}	0	4.8×10^{-7}	1
Chrysene	489779	5.1	2.5E-07	2.5×10^{-7}	0	2.4×10^{-7}	4	2.4×10^{-7}	3

Table S5. Effect of association constants of analytes (K_a^A) on the accuracy of the one calibrant equations (eq. 9).

$K_a^A \times 10^3$	$a_e \text{ min}^{-1} \times 10^2$			% Error from eq. 9 (power=1)	% Error from eq. 9
	Numerical simulation	Calculated from eq. 9 (power=1)	Calculated from eq. 9		
1	3.70	3.70	1.82	0.00	0.00
2.5	7.86	9.25	3.21	15.0	2.5
5	14.2	18.5	4.94	23.2	2.3
10	26.1	37.0	6.35	29.4	0.3
20	48.0	74.0	7.59	35.1	1.6

Table S6. Quantitative evaluation of the correspondence between the numerical model and the experimental data.

Figure #	Root mean square error (RMSE)
Figure 2 (extraction time profile)	4.12×10^{-2}
Figure 2 (desorption time profile)	5.89×10^{-2}
Figure 5 (benzene)	1.14×10^{-1}
Figure 5 (toluene)	1.36×10^{-2}
Figure 5 (ethylbenzene)	6.72×10^{-3}

$$RMSE = \sqrt{\frac{\sum (a_e (\text{numerical solution}) - a_e (\text{experimental data}))^2}{\text{number of data points}}}$$

References

- (1) Ouyang, G.; Cui, S.; Qin, Z.; Pawliszyn, J. *Anal. Chem.* **2009**, *81*, 5629–5636.
- (2) Cui, X.; Bao, L.; Gan, J. *Environ. Sci. Technol.* **2013**, *47*, 9833-9840.
- (3) Vrana, B.; Mills, G. A.; Dominiak, E.; Greenwood, R. *Environ. Pollut.* **2006**, *142*, 333-343.